NASA TECHNICAL NOTE

NASA TN D-6437

NASA TN D-6437

PRELIMINARY SECTOR TESTS AT 920 K (1200° F) OF THREE AFTERBURNER CONCEPTS APPLICABLE FOR HIGHER INLET TEMPERATURES

by Gregory M. Reck, J. Robert Branstetter, and Larry A. Diehl

Lewis Research Center
Cleveland, Ohio 44135

NATIONAL AERONAUTICS AND SPACE ADMINISTRATION • WASHINGTON, D. C. • AUGUST 1971

1. Report No.	2. Government Accession No.	3. Recipient's
NASA TN D-6437		

4. Title and Subtitle	5. Report Date
PRELIMINARY SECTOR TESTS AT 920 K (1200° F) OF THREE AFTERBURNER CONCEPTS APPLICABLE FOR HIGHER INLET TEMPERATURES	August 1971
	6. Performing Organization Code
7. Author(s)	8. Performing Organization Report No.
Gregory M. Reck, J. Robert Branstetter, and Larry A. Diehl	E-6057
	10. Work Unit No.
9. Performing Organization Name and Address	720-03
Lewis Research Center National Aeronautics and Space Administration Cleveland, Ohio 44135	11. Contract or Grant No.
	13. Type of Report and Period Covered
12. Sponsoring Agency Name and Address	Technical Note
National Aeronautics and Space Administration Washington, D.C. 20546	14. Sponsoring Agency Code

15. Supplementary Notes

16. Abstract

Three afterburner flameholder concepts proposed for 1260 K (1800° F) inlet temperature were tested, and the results were compared with a conventional V-gutter flameholder. Tests of carbureting V-gutters, film vaporizing V-gutters, and swirl-can arrays were conducted in a 49-cm (19.3-in.) diameter duct with vitiated inlet air at 920 K (1200° F), a velocity of 150 m/sec (500 ft/sec), and a pressure of 10.0 N/cm^2 (14.5 psia). Features of these designs included fuel-cooled flameholder surfaces for increased durability and premixed fuel-air systems to extend blowout limits. Carbureting V-gutters and film vaporizing V-gutters cooled the flameholder surfaces and extended the lean blowout limits relative to a conventional V-gutter. Swirl-can arrays also demonstrated an improvement in lean blowout performance. Combustion efficiency and total-pressure loss of all three flameholder concepts were comparable to a conventional V-gutter.

17. Key Words (Suggested by Author(s))

Afterburner
V-gutter
Swirl-can
Flameholder
Thrust augmentation
Combustion efficiency

18. Distribution Statement

Unclassified - unlimited

19. Security Classif. (of this report)	20. Security Classif. (of this page)	21. No. of Pages	22. Price*
Unclassified	Unclassified	41	$3.00

*For sale by the National Technical Information Service, Springfield, Virginia 22151

PRELIMINARY SECTOR TESTS AT 920 K (1200° F) OF THREE AFTERBURNER CONCEPTS APPLICABLE FOR HIGHER INLET TEMPERATURES

by Gregory M. Reck, J. Robert Branstetter, and Larry A. Diehl

Lewis Research Center

SUMMARY

Sector configurations of three afterburner flameholder concepts applicable for 1260 K (1800° F) inlet temperature operation were compared with a conventional V-gutter flameholder. Tests of carbureting V-gutters, film vaporizing V-gutters, and swirl-can arrays were conducted in a 49-centimeter (19.3-in.) diameter duct with vitiated inlet air at 920 K (1200° F), a velocity of 150 meters per second (500 ft/sec), and a pressure of 10.0 newtons per square centimeter (14.5 psia). Features of these designs included fuel-cooled flameholder surfaces for increased durability and premixed fuel-air systems to extend lean blowout by providing locally high fuel-air ratios at the V-gutter lip. Carbureting V-gutters and film vaporizing V-gutters cooled the flameholder surfaces and improved the lean blowout performance relative to a conventional V-gutter. Swirl-can arrays also demonstrated an improvement in lean blowout performance. Combustion efficiency and total-pressure-loss data for all three were comparable to a conventional V-gutter. Several versions of each concept showed the effect of design variations on performance.

INTRODUCTION

The application of conventional afterburner technology to modern turbojet engines is complicated by the current trend toward higher turbine discharge temperatures (ref. 1). As the afterburner inlet temperature exceeds 1140 K (1600° F), severe component endurance problems are encountered which indicate a need for new design concepts. In addition, there is a growing interest in afterburner operation over an extended range of fuel-air ratios. Neither improved durability nor widened operating limits should be obtained at the expense of satisfactory ignition, good combustion efficiency, or minimum pressure loss.

This report presents a preliminary screening program conducted at the Lewis Research Center to evaluate the feasibility of three afterburner concepts proposed for high-temperature operation and broad stability limits. In two of the three concepts fuel is injected and mixed with air inside the flameholder. The mixture exits at the V-gutter lip. This process has several beneficial effects. The fuel cools the flameholder surfaces and in so doing undergoes evaporation. Proper control of the fuel-air mixture preparation encourages smooth combustion at very small values of overall fuel-air ratio. These two concepts are designated herein as carbureting V-gutters and film vaporizing V-gutters. The carbureting V-gutter has a very long internal passageway. The resultant large residence time coupled with the high inlet temperatures anticipated in future afterburners may be sufficient for spontaneous ignition. Both the carbureting V-gutters and the film vaporizing V-gutters utilize additional fuel injection upstream of the flameholder to extend operation to high fuel-air ratios.

The third afterburner concept, designated as swirl-can arrays, is an extension of a modular primary combustor concept developed at the Lewis Research Center (refs. 2 to 4). In reference 3, individual swirl-can modules demonstrated low lean blowout limits and good combustion efficiencies at small values of fuel-air ratio. Fuel injected in the swirl-can carburetor is expected to cool a portion of the module. Connecting V-gutters, considered necessary for cross firing purposes, contain no cooling features but their total projected area is small and hence amenable to cooling.

SCOPE OF INVESTIGATION

This investigation was conducted to evaluate on a preliminary basis the performance of three afterburner concepts and to compare each with a conventional V-gutter design. All three concepts were intended for operation with inlet temperatures as high as 1260 K (1800° F); however, the tests reported herein were conducted at 920 K (1200° F) because of facility limitations. To avoid scaling considerations, each test configuration represented a modified sector of a full-scale afterburner (i.e., similar width, spacing, and blockage). Several versions of each concept were tested; however, the designs tested were not necessarily optimum.

The performance of each afterburner configuration was evaluated and compared with the performance of a conventional V-gutter on the basis of

(1) Durability, as indicated by post-run observations of the test hardware and data from thermocouples on the flameholder surfaces

(2) Stability, as indicated by lean and/or rich blowout limits

(3) Combustion efficiency over a range of fuel-air ratios

(4) Isothermal (nonafterburning) total-pressure loss

(5) Observations of combustion resonance (screech) in the afterburner

(No attempt was made to suppress screech.)

Tests were conducted with the afterburner configurations using unheated ASTM A-1 fuel in a 49-centimeter (19.3-in.) diameter connected-duct facility. A direct-fired preheater consisting of four J-57 combustor cans fueled with clear gasoline delivered 920 K (1200° F) vitiated air to the afterburner inlet. The afterburner length was established by a set of water spraybars, located 130 centimeters (51 in.) from the afterburner inlet, which quenched the reaction. The details of the test facility and instrumentation are included in appendixes A and B, respectively.

With the exception of the swirl-can modules which were fabricated from a high-temperature nickel-chromium-iron alloy, all afterburner components were fabricated from 304 stainless steel.

TEST PROCEDURE

All tests were conducted with afterburner-inlet conditions as follows:

Total temperature, K (°F)	920 (1200)
Static pressure, N/cm^2 (psia)	10.0 (14.5)
Velocity, m/sec (ft/sec)	150 (500)
Preheater fuel-air ratio	0.012
Preheater-inlet total temperature, K (°F)	450 (350)

The resulting nominal airflow rate was 11 kilograms per second (25 lb/sec). Isothermal total pressure loss data were taken at these inlet conditions, which correspond to a Mach number of 0.27.

Testing was done in the following manner: Afterburner ignition was accomplished by momentarily increasing the fuel flow to the direct-fired preheater. After ignition, afterburner-inlet static pressure was maintained constant for various fuel flow-rate settings by adjusting the exhaust butterfly valve described in appendix A. Performance data were taken over a range of fuel-air ratios. When two zones of fuel injection were used, fuel flow to one zone was held constant while flow to the second zone was varied. Then, flow to the first zone was adjusted to a new value and the process was repeated, thereby generating a family of performance curves. Blowout points were determined by slowly raising (or lowering) afterburner fuel flow until the rich (or lean) flameout occurred. Blowout was detected by a decrease in either combustor pressure or temperature at the enthalpy balance exit plane.

Combustion efficiency was calculated using an enthalpy balance technique which required that no liquid water be present at the enthalpy balance plane. To ensure this, steady afterburner operation was established, then the quench-water flow rate was reduced until the average temperature at the enthalpy balance plane exceeded 700 K (800° F). This temperature value was selected on the basis of experience, which showed the calculated value of combustion efficiency to be invariant for a range of average temperatures from 700 to beyond 867 K (800° to 1100° F). Data used for calculation of combustion efficiency were obtained only after the system reached thermal equilibrium.

CALCULATIONS

Afterburner Fuel-Air Ratio, Unburned

To include the effects of vitiation of the inlet air and incomplete combustion in the preheater, the afterburner fuel-air ratio, unburned, is computed by dividing the total fuel flow available to the afterburner by the available unburned airflow. Further discussion is included in appendix C.

Inlet Velocity and Mach Number

Both inlet velocity and Mach number are average values calculated from the measured airflow rate, the inlet reference area of the afterburner test section, the average inlet total temperature, and the inlet static pressure. The inlet reference area of the afterburner test section was 1878 square centimeters (291 in.^{2}).

Total-Pressure Loss

The afterburner total-pressure loss is defined as

$$\frac{\Delta P}{P} = \frac{\text{Inlet total pressure - Average exit total pressure}}{\text{Inlet total pressure}}$$

where the inlet total pressure is an average value calculated from the inlet static pressure and the Mach number.

Combustion Efficiency

Combustion efficiency is defined as the ratio of the heat output of the afterburner to the chemical energy of all fuel entering the afterburner. Heat-transfer losses from the duct components and the vitiating effect of the direct-fired preheater are included in the calculation. The heat-transfer losses consist of measured losses from the water-cooled combustion section and estimated radiation losses from the enthalpy balance section. The sum of these losses amounts to 23 to 35 joules per gram of air (10 to 15 Btu/lb of air). The combustion efficiency equation and its derivation are included in appendix C.

The value of afterburner inlet temperature used in the calculation of afterburner combustion efficiency is computed from the preheater inlet-air temperature, the preheater fuel-air ratio, the estimated heat losses from duct components, and the preheater combustion efficiency. This procedure was necessary because the ignition technique was damaging to the afterburner inlet thermocouples (see appendix B). For the operating condition used in these tests, the preheater combustion efficiency was taken to be 97 percent, a value substantiated on several occasions by analysis of the composition of the preheater exhaust gases.

Blocked Area

The value of blocked area associated with each configuration is defined as the ratio of the projected frontal area to the inlet reference area of the afterburner test section.

Units

The U.S. customary system of units was used for primary measurements and calculations. Conversion to SI units (Systeme International d'Unites) is done for reporting purposes only. In making the conversion, consideration is given to implied accuracy and may result in rounding off the value expressed in SI units.

REFERENCE V-GUTTER AFTERBURNERS

Purpose

Reference V-gutter configurations have been included in this report for comparison purposes only. The data comparisons were made at 920 K (1200° F), which is well below

the maximum inlet temperature intended for the three concepts described in the INTRODUCTION. However, afterburner concepts applicable for high-inlet-temperature operation should perform as well as conventional V-gutter configurations when both are compared at customary inlet temperatures.

Since facility limitations precluded the use of a "full-sized" cylindrical afterburner, each test configuration represented a modified sector of a full-scale design. To establish the merit of this technique, three reference V-gutter configurations each representing a common variation in fuel injector - flameholder arrangement were tested. The results are presented herein. The three designs are considered typical of current afterburner practice and were derived from the data and design guidelines of reference 5.

Combustor Description

Details of the three reference configurations are shown in figure 1 and one of the V-gutters is shown in figure 2. In each configuration fuel is injected normal to the airflow and the fuel spraybars are 46 centimeters (18 in.) upstream of the flameholders. Configuration A-1 (fig. 1(a)) differs from configuration A-2 (fig. 1(b)) only in the relative orientation of the fuel spraybars and V-gutter flameholders. A parallel arrangement, as in configuration A-1, represents a full-scale afterburner design with circular V-gutters and fuel sprayrings. A perpendicular arrangement, as in configuration A-2, represents a full-scale design with circular V-gutters and radial fuel spraybars. The A-3 flameholder (fig. 1(c)), while having nearly the same total blockage as configurations A-1 and A-2, has three instead of four gutters. Also, figure 1(c) shows the A-3 spraybars mounted in line with the V-gutters, whereas figure 1(a) shows the A-1 spraybars mounted between the V-gutters. In each configuration, the fuel flow control to the middle spraybar is independent of the flow control to the combined side spraybars.

Results and Discussion

Several aspects of the performance of the V-gutter configurations are shown in figures 3 and 4. Figure 3(a) illustrates how the combustion efficiency curve for each configuration is generated. The locus curve is the maximum combustion efficiency with any fuel-air ratio combination distributed among the spraybars. The combustion efficiency data, blowout data, and pressure loss data, all of which are shown in figure 3, are comparable with full-scale data from reference 5. It is interesting to note that longitudinal screech at 200 hertz was observed with configurations A-1 (fig. 3(a)) and A-2 (fig. 3(b)). Figure 4 shows that V-gutter temperatures are near the value of the afterburner inlet temperature for all values of fuel-air ratio, unburned.

For the purpose of comparison in this report, configuration A-1 is referred to as the "reference" configuration, and the locus of maximum combustion efficiency for this configuration is included with combustion efficiency data of the other configurations.

CARBURETING V-GUTTERS

Combustor Description

The carbureting V-gutter demonstrates one method of improving flameholder durability at high inlet temperatures by fuel-cooling the flameholder surfaces. Fuel is injected and mixed with air at the carburetor inlet and undergoes two flow turns and a long flow passageway before exiting at the V-gutter lip. Cross-sectional views of two versions of this design concept are shown in figure 5. The second version, configuration B-2, is designed with a narrower V-gutter than configuration B-1. Hence, the two versions differ in internal flow characteristics and combustor total-pressure loss. Identical flameholder fuel spraybars are used for both designs and are shown in figure 6. When needed, additional fuel is injected 41 centimeters (16 in.) upstream of the carburetor inlets using the spraybars shown in figure 7. Both the flameholder fuel spraybars and the upstream fuel spraybars inject normal to the airflow. Figure 8 is a view, looking downstream, of the carburetor for configuration B-2.

Results and Discussion

The performance of both carburetor designs is shown in figure 9. Configuration B-1 provided combustion efficiencies comparable to those of the reference V-gutter, however, the efficiencies of configuration B-2 were lower. Both designs demonstrated lean blowout limits lower than that of the reference V-gutter. Configuration B-1 produced higher total-pressure losses than the reference V-gutter, whereas configuration B-2 with a narrower V-gutter produced pressure losses comparable to the reference V-gutter. At the inlet air temperatures tested, no spontaneous ignition was observed with either configuration.

Figure 10 shows temperature data from thermocouples mounted on the upstream surface of the V-gutter. The data indicate the effectiveness of fuel-cooling in the carburetor and suggest that a significant improvement in durability may be achieved with this design.

FILM VAPORIZING V-GUTTER

Combustor Description

The film vaporizing V-gutter can improve afterburner durability at high inlet temperatures by fuel-cooling the flameholder surfaces. Five versions of this flameholder are shown in figure 11. The variations are arbitrary and are made to demonstrate the significance of geometry and resultant flow behavior on performance. Configurations C-1 and C-2 differ only in flameholder length and the exit area available to the airflow through the flameholder. Configuration C-3 is a modification of C-1 in which the flameholder fuel-air mixture is not ducted to the V-gutter lip. Configuration C-4 is a modification of C-2 in which the flameholder fuel-air mixture is ducted past the V-gutter lip. Finally, configuration C-5 is similar in shape to C-1 and C-2, but with increased V-gutter width. The flameholder fuel spraybars are identical for all five designs and are shown in figure 6. When needed, additional fuel is injected 41 centimeters (16 in.) upstream of the flameholder inlet using the spraybars shown in figure 12. All fuel is injected normal to the airflow. A typical film vaporizing V-gutter installation is shown in figure 13.

Results and Discussion

The combustion efficiency and stability data shown in figure 14 for the film vaporizing V-gutters indicates that configurations C-1, C-2, and C-3 performed as well as, or better than, the reference V-gutter configuration, while configurations C-4 and C-5 showed undesirable performance characteristics. Configuration C-2 coupled high combustion efficiencies with a low lean blowout limit. Configuration C-4, which ducted the flameholder fuel-air mixture past the V-gutter lip, showed the lowest lean blowout limit; but combustion efficiencies were substantially lower than those of the reference V-gutter. Configuration C-5 showed high values of combustion efficiency, but was prone to transverse screech at values of fuel-air ratio, unburned, greater than 0.03.

The isothermal total-pressure-loss data for the film vaporizing V-gutter configurations (fig. 14) indicate a large pressure loss for the C-5 configuration. The total-pressure loss is approximately 5 to 6 percent for the remaining four configurations, which have identical blocked areas.

Post-run inspections of the film vaporizing V-gutter configurations indicated that the flameholders were well cooled. This observation was verified by data from thermocouples mounted on the upstream surface of a V-gutter. These data are shown in figure 15.

SWIRL-CAN ARRAYS

Combustor Description

In addition to problems with flameholder durability at high inlet temperatures, afterburners must operate efficiently over a wide range of fuel-air ratios. The use of swirl-can modules (with interconnecting V-gutters) can hopefully extend afterburner operation to small values of fuel-air ratio while simultaneously providing high combustion efficiencies. Interconnecting V-gutters are expected to improve ignition and crossfiring between swirl-cans. The gutters, in conjunction with upstream fuel injection, should provide good performance at high fuel-air ratios.

The swirl-can module shown in figure 16 and discussed in reference 3 is arranged in three arrays as shown in figure 17. In the first configuration, D-1, separate fuel systems supply the inner zone of four cans and the outer zone of eight cans and permit independent flow control of each zone. Configuration D-2 reduces the number of swirl-cans in the array, but maintains a blocked area ratio approximately equal to that of configuration D-1 by widening the interconnecting V-gutters. The third array, configuration D-3, is identical to D-2 except that the V-gutters are narrowed to reduce the blocked area. The swirl-can modules in configurations D-2 and D-3 are connected to a single fuel supply system. For these two designs, the effect of additional fuel injection upstream of the swirl-can array is investigated by connecting a second fuel system to the sprayrings shown in figure 18. The sprayrings are located 41 centimeters (16 in.) upstream of the swirl-can inlets. Figure 19 shows the installation of the D-3 array.

Results and Discussion

The combustion efficiency data presented in figure 20 for the swirl-can arrays show that each design performed as well as, or better than, the reference V-gutter configuration. Low lean blowout limits were observed for all three designs. The large pressure losses (fig. 20) observed for the swirl-can arrays are believed to result in part from frictional drag losses of the swirl-can fuel manifold and the swirl-can support structures.

A comparison of the performance of configuration D-1 with the performance of D-2 indicates that, with similar blocked areas and pressure losses, the larger number of swirl-can modules in configuration D-1 yielded higher combustion efficiencies. Configuration D-3 reduced the large pressure loss of configuration D-2 by trimming the interconnecting V-gutters, which resulted in only slight changes in combustion efficiencies.

PERFORMANCE COMPARISON

The locus curves of combustion efficiency for a carbureting V-gutter, a film vaporizing V-gutter, a swirl-can array, and the reference V-gutter are compared in figure 21. The configurations displayed in figure 21 were selected on the basis of overall performance, which included isothermal total-pressure loss, combustion efficiency, blowout limits, durability, and screech. The carbureting V-gutter configuration B-2 shows the lowest values of combustion efficiency; while the film vaporizing V-gutter configuration C-2 shows the highest combustion efficiency, with a peak value of 92 percent.

The isothermal total-pressure losses of all configurations tested are compared in figure 22. The reference V-gutters show the lowest total-pressure loss, with a value of 4.7 percent. Configurations B-2, C-2, and D-3 (all of which were included in fig. 21) exhibit pressure losses of 5.2 to 5.7 percent.

The effectiveness of fuel-cooling the flameholder surfaces for improved durability is indicated by data from thermocouples mounted on the upstream surface of a V-gutter. These data from a carbureting V-gutter, a film vaporizing V-gutter, and a reference V-gutter are compared in figure 23. Both the carbureting V-gutter and the film vaporizing V-gutter demonstrate improvements over the reference V-gutter.

CONCLUDING REMARKS

The results of this investigation were encouraging. The carbureting V-gutters and the film vaporizing V-gutters cooled the flameholder surfaces and can be used in high-inlet-temperature applications. These two concepts and the swirl-can arrays demonstrated improved lean blowout performance when compared to a conventional V-gutter. All three combustor types produced combustion efficiency and total-pressure-loss data comparable in value to corresponding data from a conventional V-gutter configuration.

Lewis Research Center,
National Aeronautics and Space Administration,
Cleveland, Ohio, May 6, 1971,
720-03.

APPENDIX A

TEST FACILITY

A diagram of the test facility and a view of the apparatus are presented in figures 24 and 25, respectively. The combustion air, after being heated in a natural-gas-fired, tube-type heat exchanger, flows through the measuring orifice. A choked butterfly valve regulates the flow and a perforated cylinder disperses the air into the inlet plenum (ref. 6). Further downstream, four J-57 combustor cans fueled with gasoline heat the air, with vitiation, and exhaust to the afterburner inlet. A cross-sectional view of the afterburner test section, including a conventional fuel injector and V-gutter installation, is shown in figure 26. At the exit of the afterburner, the combustion products are quenched by a set of nine water spraybars containing a total of about 200 orifices. The water is injected normal to the gas flow. Two parallel flow systems supply water to the quench spraybars and provide accurate flow control. Baffles mounted in the enthalpy balance section (fig. 27) promote mixing and vaporization of the quench water. Downstream of the enthalpy balance section (fig. 27), the gases are further quenched and flow out through the exhaust butterfly valve into the altitude exhaust system.

ASTM A-1 fuel for the afterburner is supplied through two parallel systems, each containing two flowmeters, a throttle valve, and a positive shutoff valve.

APPENDIX B

INSTRUMENTATION

Airflow rate is measured by a sharp-edged orifice with flange pressure taps installed according to ASME specifications. The location of other fixed-position pressure and temperature sensors is shown in figure 27. The temperature rakes shown in section A-A are used to monitor the quality of the afterburner inlet temperature profile.

Two turbine-type flowmeters are series-mounted in each of the two ASTM A-1 supply systems and in the gasoline supply system for the direct-fired preheater. Three turbine-type flowmeters are mounted in the water quench system, one measuring the total flow rate, and one in each of the two parallel systems delivering the water to the quench spraybars. The flow rate of the cooling water for the combustion section (fig. 27) is measured by an orifice.

Data from the steady-state instrumentation are recorded by the laboratory's automatic data recording and processing system (ref. 7). A portion of the instrumentation is connected to an analog computer which provides a continuous display in the control room of airflow rate and unburned fuel-air ratio.

Dynamic pressure transducers are located on the inlet plenum and in the afterburner inlet and exit planes shown in figure 27. These transducers are flush mounted and have their diaphragms exposed to the flow gases in order to detect the presence of acoustic resonance (screech). The outputs of these transducers are displayed in the control room and recorded on high-speed strip charts.

APPENDIX C

CALCULATION OF FUEL-AIR RATIO AND COMBUSTION EFFICIENCY

The preheater fuel-air ratio f_{ph} and the afterburner fuel-air ratio f_{ab} are calculated by dividing the respective fuel-flow rate by the total airflow rate.

The afterburner fuel-air ratio, unburned, obtained from reference 8 is

$$\text{Fuel-air ratio, unburned} = \frac{w_{ft} - \left(w_{f,ph}\eta_{ph}/100\right)}{w_a - \left(\frac{w_{f,ph}\eta_{ph}/100}{0.067}\right)}$$

where

w_{ft} total fuel-flow rate to both preheater and afterburner, kg/sec (lb/sec)

$w_{f,ph}$ preheater fuel-flow rate, kg/sec (lb/sec)

η_{ph} preheater combustion efficiency, percent

w_a total airflow rate, kg/sec (lb/sec)

The terms f_{ph} and f_{ab} are used in the calculation of combustion efficiency. The afterburner fuel-air ratio, unburned, is used only in the discussion and presentation of data.

Combustion efficiency is defined as the ratio of the heat output of the afterburner to the chemical energy of all fuel entering the afterburner. The heat output (Δh_o, J/kg (Btu/lb)) is equal to

$$\Delta h_o = \Delta h_p + \Delta h_w + q_l$$

where

Δh_p change in enthalpy of afterburner propellant fluids (fuel, air, and combustion products), J/kg (Btu/lb)

Δh_w change in enthalpy of water used to quench afterburner exhaust gases, J/kg (Btu/lb)

q_l heat losses from system, J/kg (Btu/lb)

In the calculation of Δh_p, combustion in both the preheater and the afterburner is assumed to occur at a reference temperature of 298 K (537^o R), and the products of combustion are assumed to be CO_2 and H_2O in the gaseous phase. The enthalpy (h_m, J/kg

(Btu/lb)) of a leaner-than-stoichiometric burned mixture of fuel and air may be expressed (ref. 9) as

$$h_m = \left[h_a + f\left(\frac{Am + B}{m + 1}\right) \right]_{T_r}^{T_b}$$

where, for example $\left[h_a\right]_{T_r}^{T_b}$ is used to mean "the value of h_a at T_b minus the value of h_a at T_r," and where

h_a enthalpy of air, J/kg (Btu/lb)

f fuel-air ratio

T_r reference temperature equal to 298 K (537° R)

T_b total temperature of burned mixture, K (°R)

m hydrogen-carbon ratio of fuel

$$A = \frac{H_{H_2O} - \frac{1}{2} H_{O_2}}{2.016}$$

$$B = \frac{H_{CO_2} - H_{O_2}}{12.010}$$

and

H molal enthalpy, J/mole (Btu/mole)

The term (Am + B)/(m + 1) accounts for the difference between the enthalpy of the carbon dioxide and water vapor in the burned mixture and the enthalpy of the oxygen removed from the air by their formation.

The expression for h_m may be used to determine the enthalpy of the gases entering the afterburner from the preheater, as well as the enthalpy of the afterburner combustion products. However, prior to expressing Δh_p in terms of h_m, we should bear in mind that (1) the combustion efficiency of the preheater is assumed to be 97 percent, (2) the enthalpy of the unburned gasoline entering the afterburner from the preheater is considered negligible, and (3) the enthalpy of the ASTM A-1 fuel is zero, since this fuel is assumed to enter the afterburner at the reference temperature. Finally, the change in enthalpy of the afterburner propellant fluids becomes

$$\Delta h_p = \left[h_a + f_{ph} \left(\frac{As + B}{s + 1} \right) + f_{ab} \left(\frac{Ar + B}{r + 1} \right) \right]_{T_r}^{T_{bal}} - \left[h_a + f_{ph} \left(\frac{As + B}{s + 1} \right) \right]_{T_r}^{T_{in}}$$

$$= \left[h_a + f_{ph} \left(\frac{As + B}{s + 1} \right) \right]_{T_{in}}^{T_{bal}} + \left[f_{ab} \left(\frac{Ar + B}{r + 1} \right) \right]_{T_r}^{T_{bal}}$$

where

f_{ph} fuel-air ratio of preheater

s hydrogen-carbon ratio of preheater fuel

f_{ab} fuel-air ratio of afterburner

r hydrogen-carbon ratio of afterburner fuel

T_{bal} total temperature at enthalpy balance plane, K (^{o}R)

T_{in} total temperature at afterburner inlet, K (^{o}R)

The change in enthalpy of the quench water Δh_w was computed by assuming that no liquid water is present at the enthalpy balance plane. The expression is as follows

$$\Delta h_w = \left[\frac{w_q}{w_a} h_w \right]_{T_{w,in}}^{T_{bal}}$$

where

w_q quench-water flow rate, kg/sec (lb/sec)

w_a airflow rate, kg/sec (lb/sec)

h_w enthalpy of water, J/kg (Btu/lb)

$T_{w,in}$ temperature of quench water entering afterburner, K (^{o}R)

The heat losses from the system q_l are calculated for two duct components, the water-cooled combustion section and the enthalpy balance tube. The heat losses are expressed as

$$q_l = \frac{w_{cw}}{w_a} \left(T_{cw,out} - T_{cw,in} \right) + \frac{C}{w_a} \left(T_{bal} \right)^4$$

where

w_{cw} cooling-water flow rate, kg/sec (lb/sec)

$T_{cw,out}$ cooling-water outlet temperature, K (^{o}R)

$T_{cw,in}$ cooling-water inlet temperature, K (^{o}R)

C empirical radiation heat-transfer constant, 2.13×10^{-7} J/sec K^4 (1.92×10^{-11} Btu/sec $^{o}R^4$)

The expression for the total heat output is now

$$\Delta h_o = \left[h_a + f_{ph}\left(\frac{As + B}{s + 1}\right)\right]_{T_{in}}^{T_{bal}} + \left[f_{ab}\left(\frac{Ar + B}{r + 1}\right)\right]_{T_r}^{T_{bal}}$$

$$+ \left[\frac{w_q}{w_a} h_w\right]_{T_{w,in}}^{T_{bal}} + \frac{w_{cw}}{w_a}\left(T_{cw,out} - T_{cw,in}\right) + \frac{C}{w_a}\left(T_{bal}\right)^4$$

The expression for the chemical energy (h_c, J/kg (Btu/lb)) of all fuel entering the afterburner includes the unburned fuel entering the afterburner from the preheater and is written as

$$h_c = \left(1 - \frac{\eta_{ph}}{100}\right) f_{ph} h_{lv,ph} + f_{ab} h_{lv,ab}$$

where

η_{ph} combustion efficiency of preheater, percent

$h_{lv,ph}$ lower heating value of preheater fuel at T_r, J/kg (Btu/lb)

$h_{lv,ab}$ lower heating value of afterburner fuel at T_r, J/kg (Btu/lb)

Now, the combustion efficiency, obtained by dividing the heat output of the afterburner Δh_o by the chemical energy of the available fuel h_c, is

$$\text{Combustion efficiency} = \left\{ \frac{\left[h_a + f_{ph}\left(\frac{As + B}{s + 1}\right) \right]_{T_{in}}^{T_{bal}} + \left[f_{ab}\left(\frac{Ar + B}{r + 1}\right) \right]_{T_r}^{T_{bal}}}{\left(1 - \frac{\eta_{ph}}{100}\right) f_{ph} h_{lv,ph} + f_{ab} h_{lv,ab}} \right.$$

$$\left. + \frac{\left[\frac{w_q}{w_a} h_w \right]_{T_{w,in}}^{T_{bal}} + \frac{w_{cw}}{w_a}\left(T_{cw,out} - T_{cw,in}\right) + \frac{C}{w_a}\left(T_{bal}\right)^4}{\left(1 - \frac{\eta_{ph}}{100}\right) f_{ph} h_{lv,ph} + f_{ab} h_{lv,ab}} \right\} \times 100$$

The thermodynamic values used in the calculation of combustion efficiency are

Hydrogen-carbon ratio of the afterburner fuel, r	0.161
Hydrogen-carbon ratio of the preheater fuel, s	0.178
Lower heating value of preheater fuel at T_r, $h_{lv,ph}$, J/kg (Btu/lb)	43 920 (18 900)
Lower heating value of afterburner fuel at T_r, $h_{lv,ab}$, J/kg (Btu/lb)	43 230 (18 600)

REFERENCES

1. Curry, John J.: Requirements for Advancement of Technology, Thrust Augmentation Systems. Rep. NAPTC-ATD-173, Naval Air Propulsion Test Center, 1969.

2. Butze, Helmut F.; Trout, Arthur M.; and Moyer, Harry M.: Performance of Swirl-Can Turbojet Combustors at Simulated Supersonic Combustor-Inlet Conditions. NASA TN D-4996, 1969.

3. Niedzwiecki, Richard W.; and Jones, Robert E.: Combustion Stability of Single Swirl-Can Combustor Modules Using ASTM-A1 Liquid Fuel. NASA TN D-5436, 1969.

4. Niedzwiecki, Richard W.; and Moyer, Harry M.: Performance of a Short Modular Turbojet Combustor Segment Using ASTM-A1 Fuel. NASA TN D-6167, 1971.

5. Barnett, Henry C.; and Hibbard, Robert R., eds.: Adaptation of Combustion Principles to Aircraft Propulsion. Vol. II - Combustion in Air-breathing Jet Engines. NACA RM E55G28, 1956.

6. Branstetter, J. Robert; Juhasz, Albert J.; and Verbulecz, Peter W.: Experimental Performance and Combustion Stability of a Full-Scale Duct Burner for a Supersonic Turbofan Engine. NASA TN D-6163, 1971.

7. Staff of the Lewis Laboratory: Central Automatic Data Processing System. NACA TN 4212, 1958.

8. King, Charles R.: Experimental Investigation of Effects of Combustion-Chamber Length and Inlet Total Temperature, Total Pressure, and Velocity on Afterburner Performance. NACA RM E57C07, 1957.

9. Turner, L. Richard; and Lord, Albert M.: Thermodynamic Charts for the Computation of Combustion and Mixture Temperatures at Constant Pressure. NACA TN 1086, 1946.

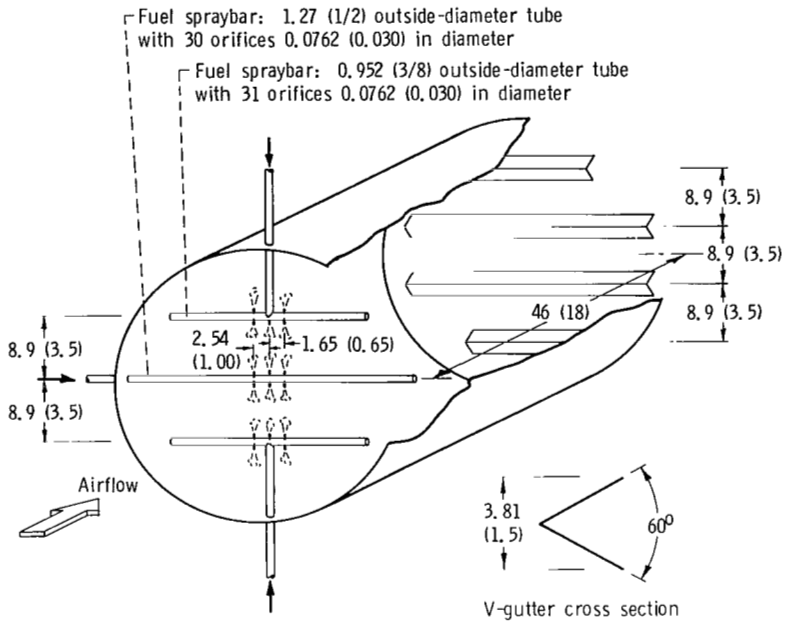

(a) Configuration A-1; blocked area ratio, 0.31.

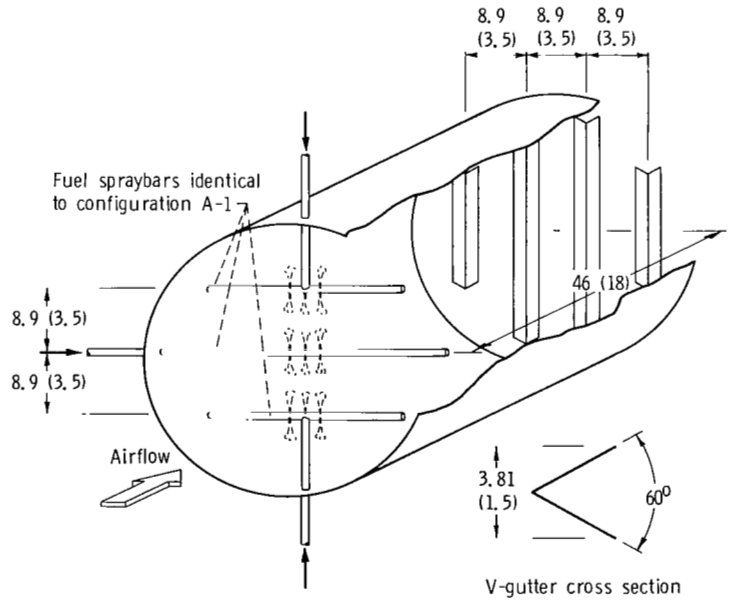

(b) Configuration A-2; blocked area ratio, 0.31.

Figure 1. - Reference V-gutter configurations. Dimensions are in centimeters (in.).

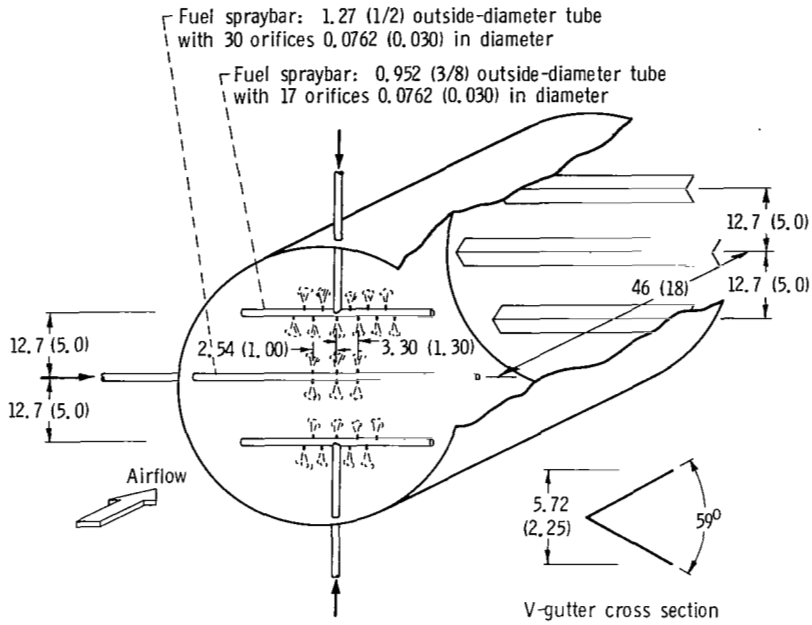

(c) Configuration A-3; blocked area ratio, 0.34.

Figure 1. - Concluded.

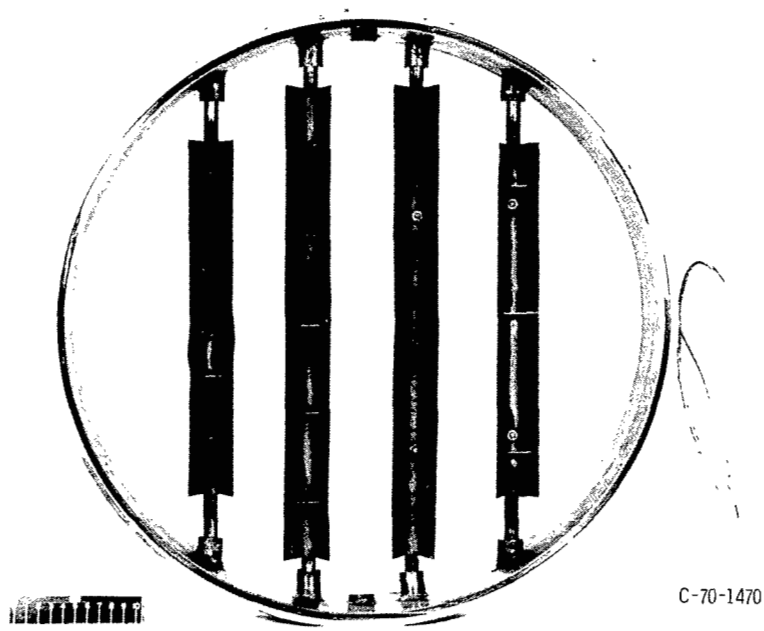

Figure 2. - Flameholder from configurations A-1 and A-2 (looking upstream).

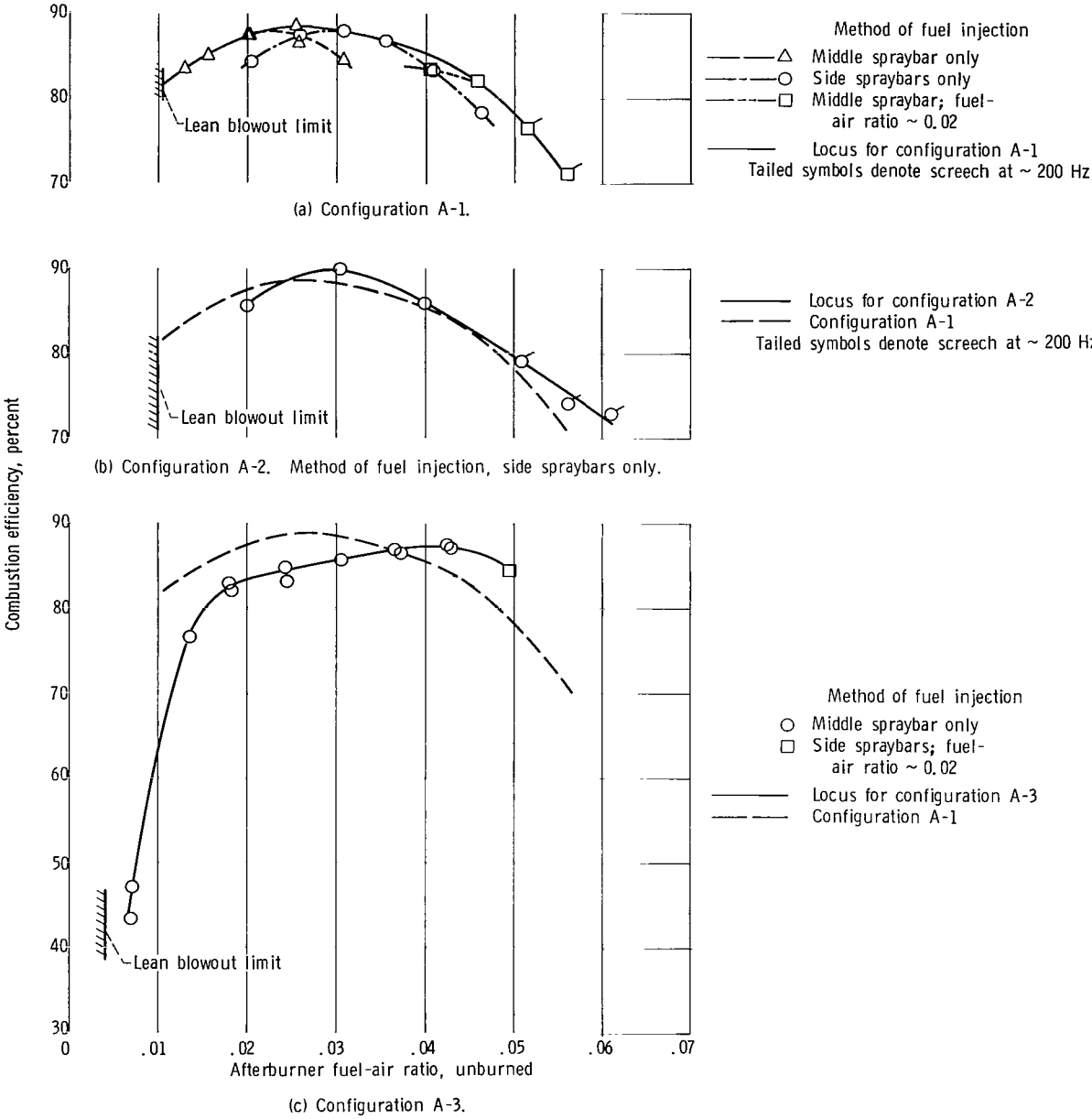

Figure 3. - Combustion efficiency of reference V-gutter afterburners. Isothermal total-pressure losses, 4.7 percent. Inlet conditions: temperature, 920 K (1200° F); pressure, 10.0 newtons per square centimeter (14.5 psia); velocity, 150 meters per second (500 ft/sec); preheater fuel-air ratio, 0.012.

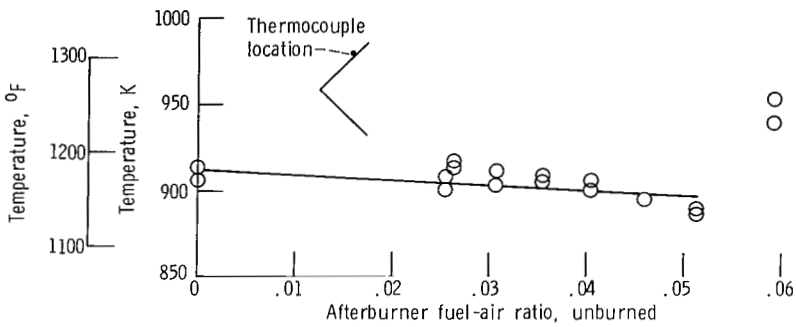

Figure 4. - V-gutter skin temperatures for reference V-gutter configuration A-1.

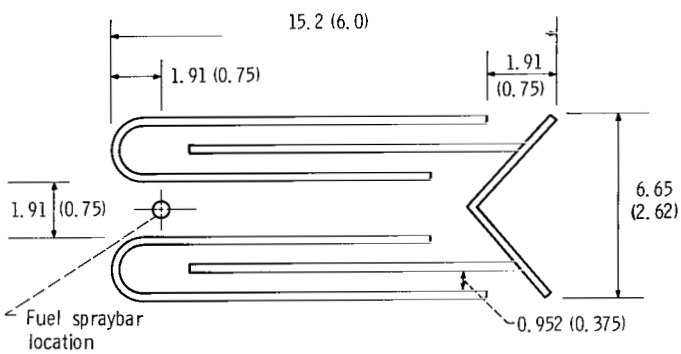

(a) Configuration B-1; blocked area ratio, 0.34.

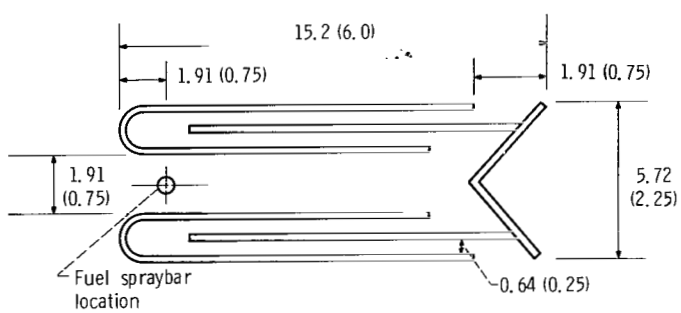

(b) Configuration B-2; blocked area ratio, 0.30.

Figure 5. - Cross-section sketch of carbureting V-gutter designs. Dimensions are in centimeters (in.).

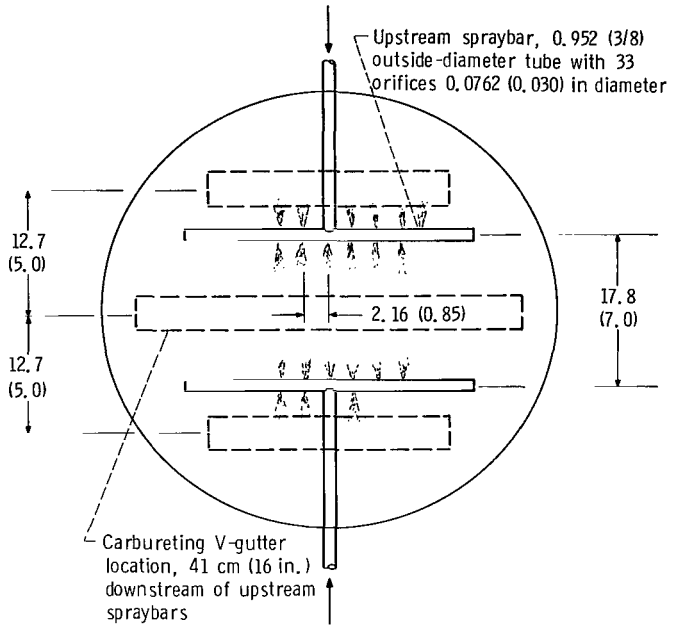

Figure 7. - Upstream fuel spraybars for carbureting V-gutter configurations. Dimensions are in centimeters (in.).

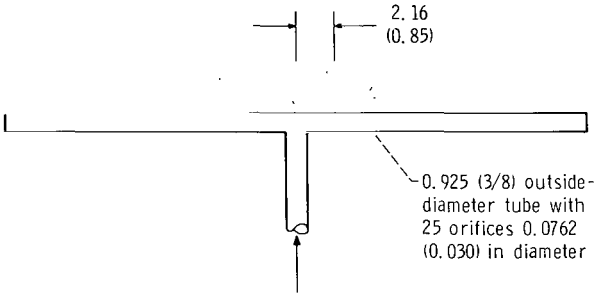

(a) Side spraybars.

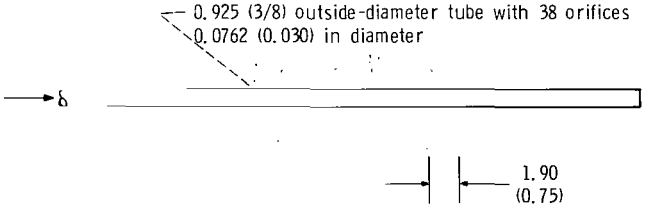

(b) Middle spraybar.

Figure 6. - Flameholder spraybar design for carbureting V-gutter and film vaporizing V-gutter configurations. Dimensions are in centimeters (in.).

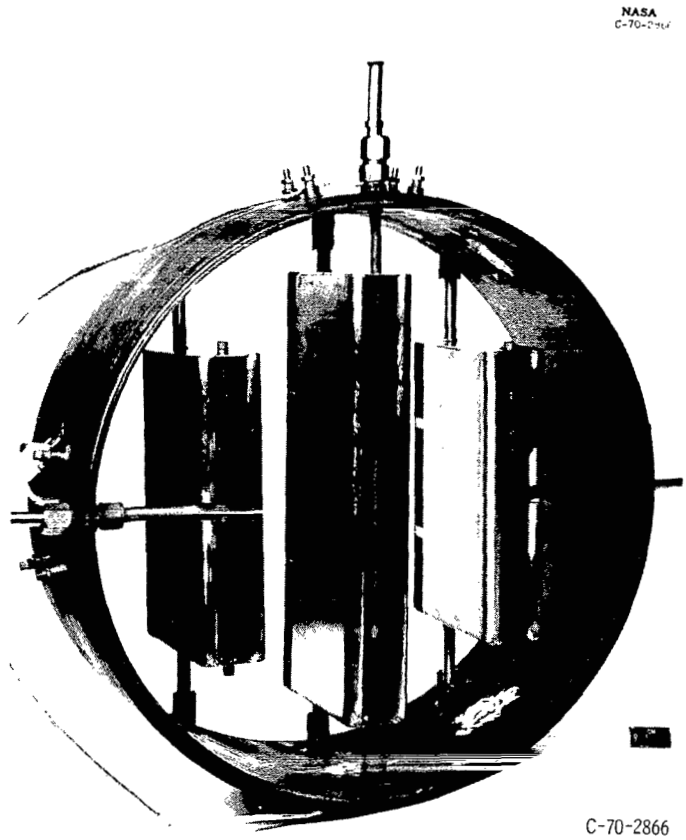

Figure 8. - Carbureting V-gutter configuration B-2 (looking downstream).

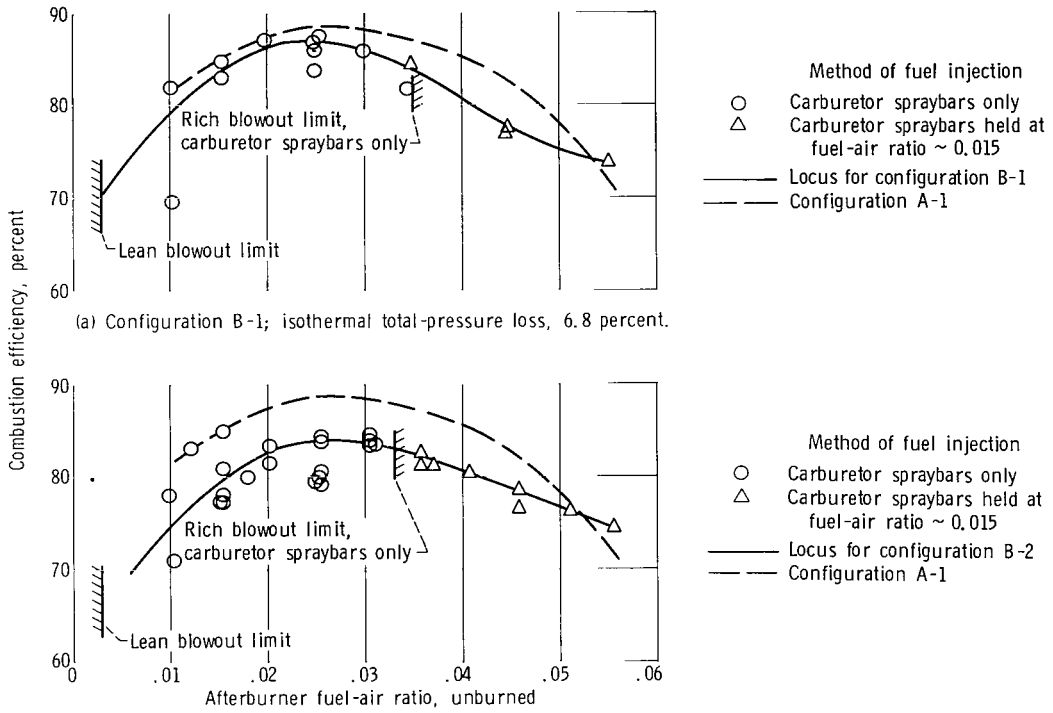

Figure 9. - Combustion efficiency of carbureting V-gutter afterburners. Inlet conditions: temperature, 920 K (1200° F); pressure, 10.0 newtons per square centimeter (14.5 psia); velocity, 150 meters per second (500 ft/sec); preheater fuel-air ratio, 0.012

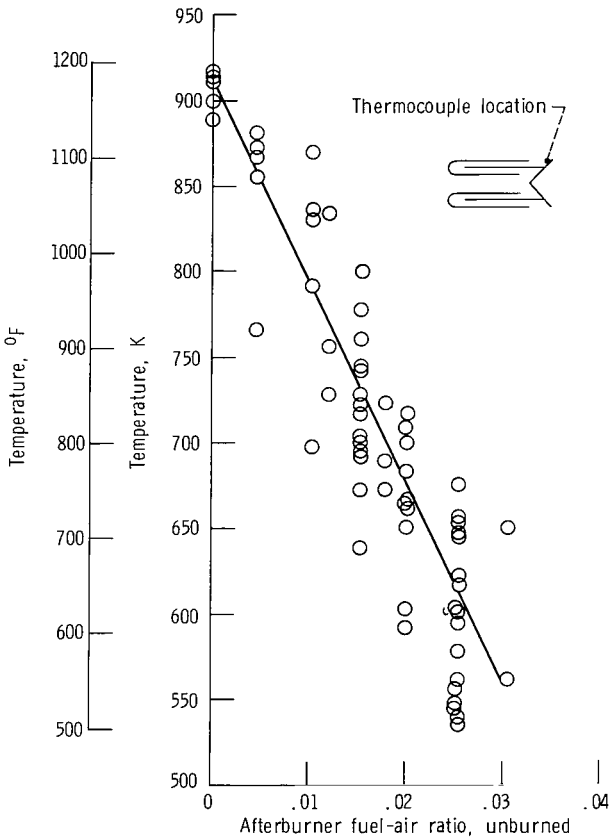

Figure 10. - V-gutter skin temperatures for carbureting V-gutter configuration B-2.

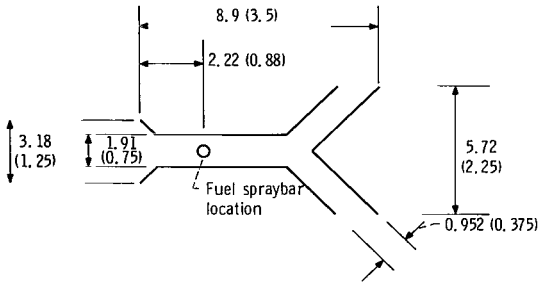

(a) Configuration C-1; blocked area ratio, 0.30.

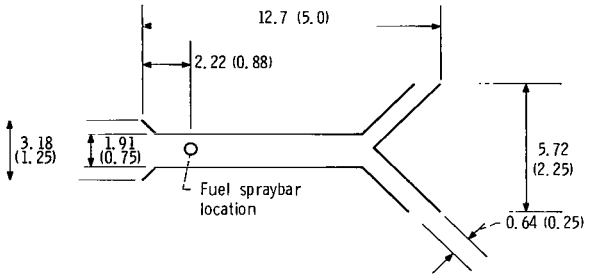

(b) Configuration C-2; blocked area ratio, 0.30.

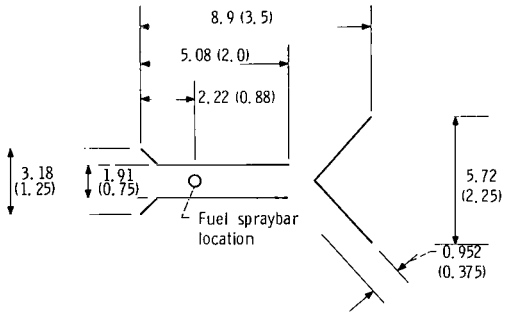

(c) Configuration C-3; blocked area ratio, 0.30.

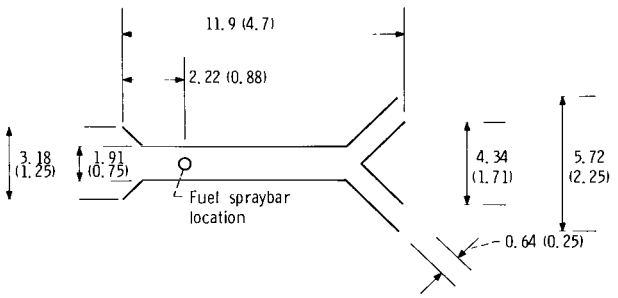

(d) Configuration C-4; blocked area ratio, 0.30.

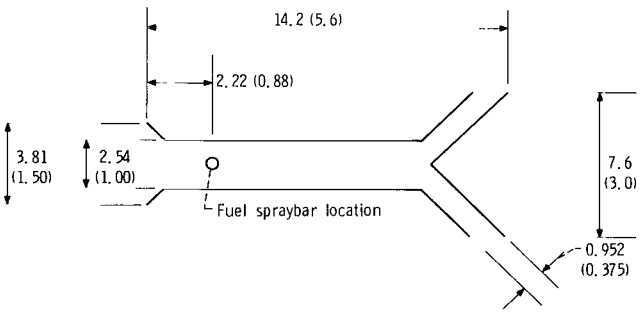

(e) Configuration C-5; blocked area ratio, 0.39.

Figure 11. - Cross-section sketches of film vaporizing V-gutter designs. Dimensions are in centimeters (in.).

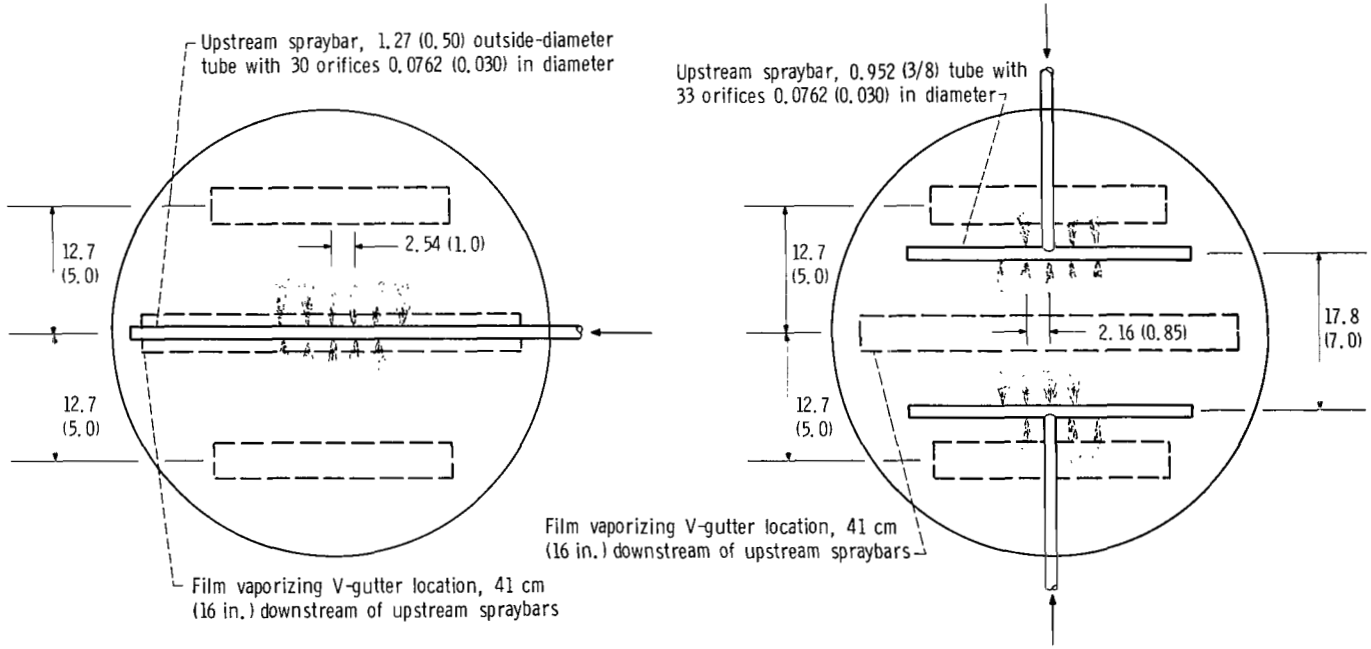

(a) Configurations C-1 and C-2.

(b) Configurations C-3, C-4, and C-5.

Figure 12. - Upstream fuel spraybar designs for film vaporizing V-gutter configurations. Dimensions are in centimeters (in.).

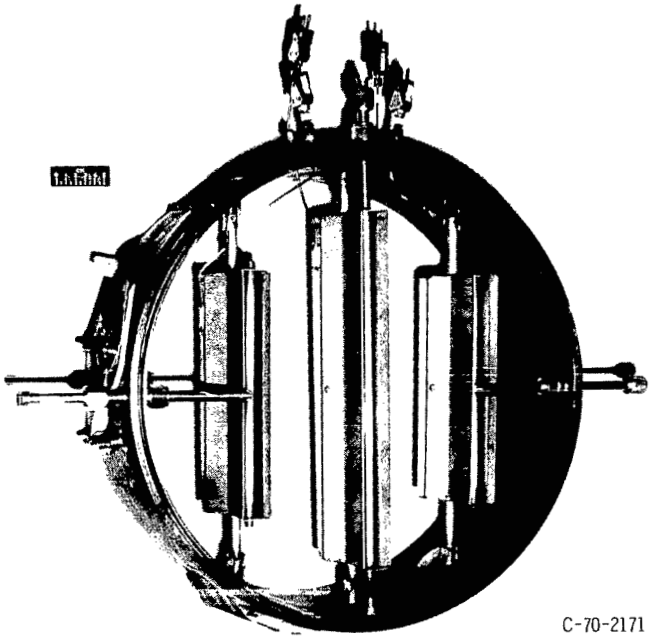

Figure 13. - Film vaporizing V-gutter configuration C-2 (looking downstream).

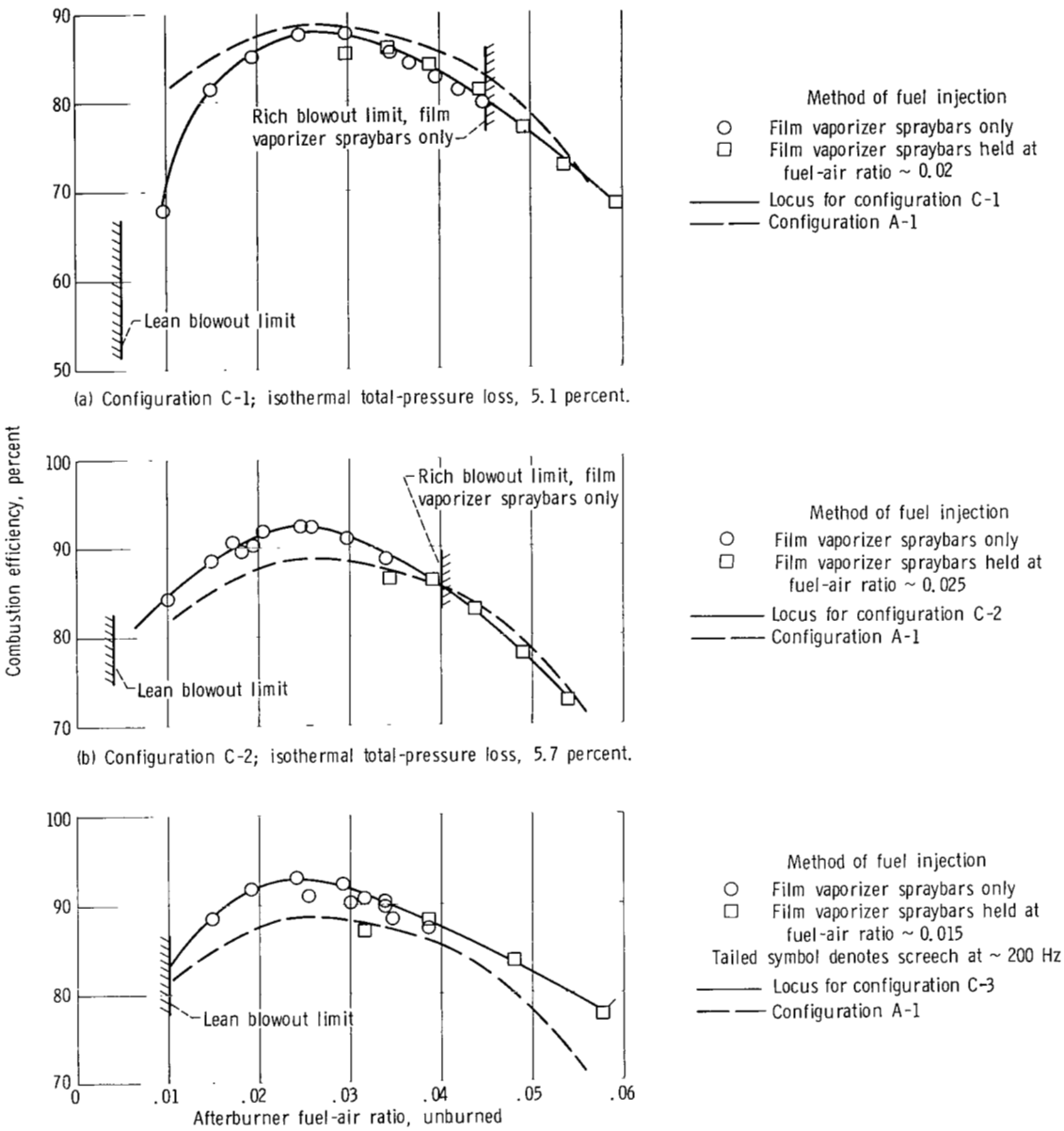

(a) Configuration C-1; isothermal total-pressure loss, 5.1 percent.

(b) Configuration C-2; isothermal total-pressure loss, 5.7 percent.

(c) Configuration C-3; isothermal total-pressure loss, 5.9 percent.

Figure 14. - Combustion efficiency of film vaporizing V-gutter afterburners. Inlet conditions: temperature, 920 K (1200° F); pressure, 10.0 newtons per square centimeter (14.5 psia); velocity, 150 meters per second (500 ft/sec); preheater fuel-air ratio, 0.012.

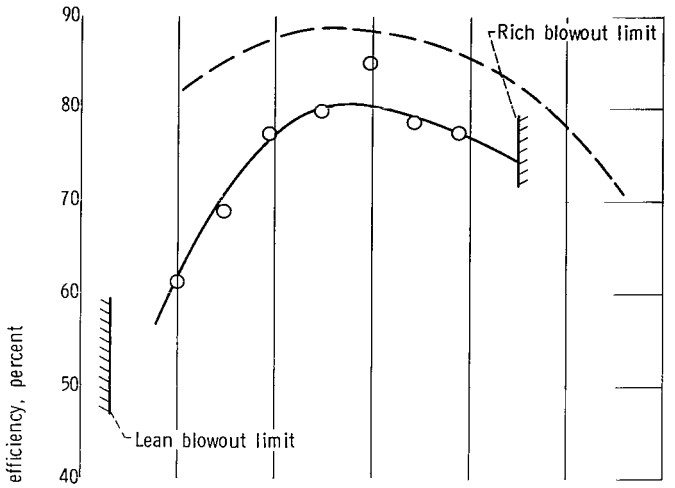

(d) Configuration C-4; isothermal total-pressure loss, 5.3 percent. Method of fuel injection, film vaporizer spraybars only.

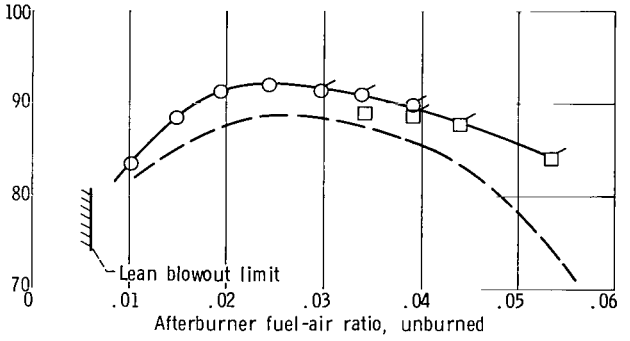

(e) Configuration C-5; isothermal total-pressure loss, 9.4 percent.

Figure 14. - Concluded.

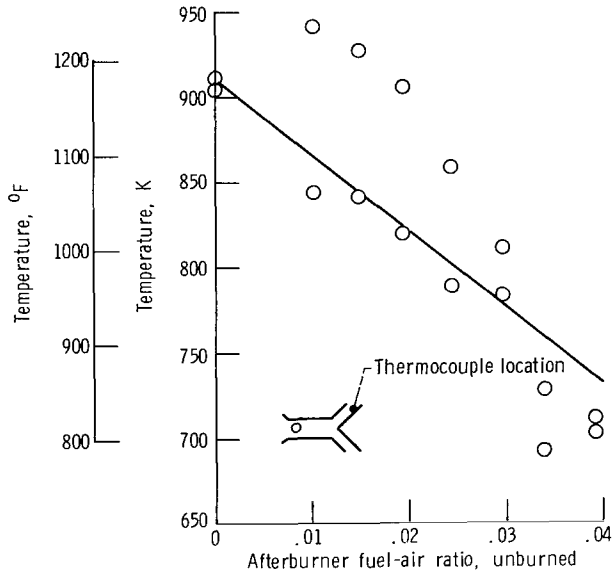

Figure 15. - V-gutter skin temperatures for film vaporizing V-gutter configuration C-5.

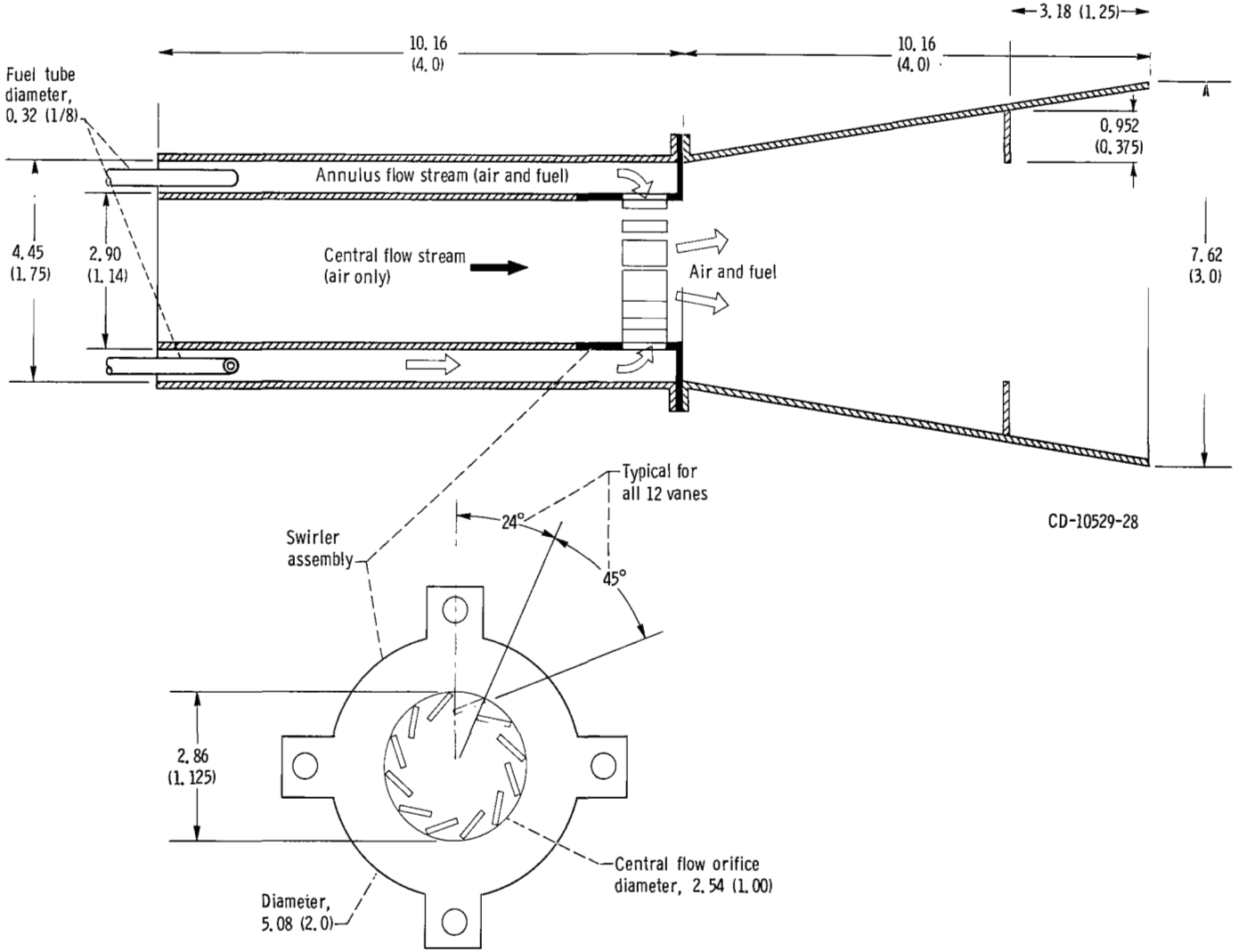

Figure 16. - Swirl-can module used in configurations D-1, D-2, and D-3. Dimensions are in centimeters (in.).

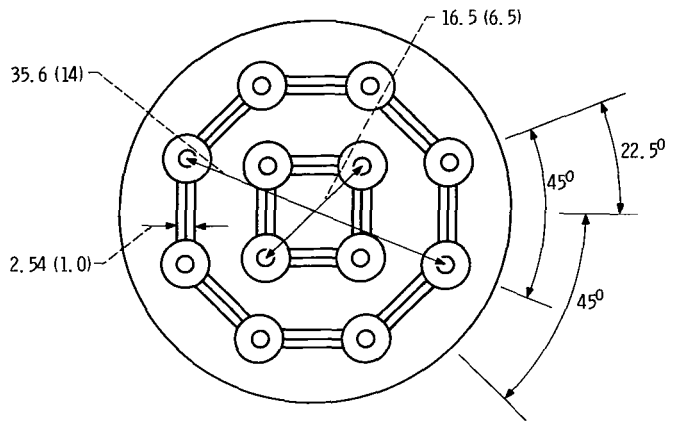

(a) Configuration D-1; blocked area ratio, 0.35.

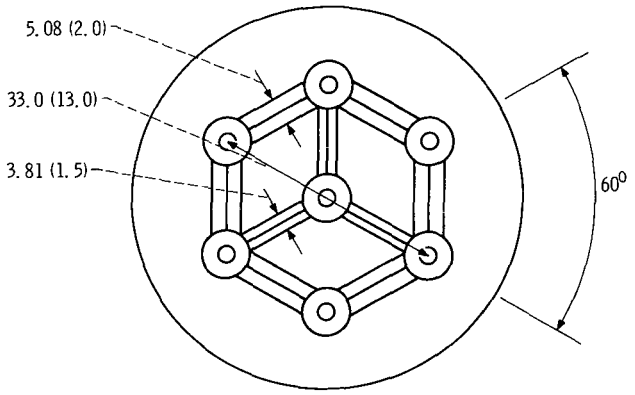

(b) Configuration D-2; blocked area ratio, 0.36.

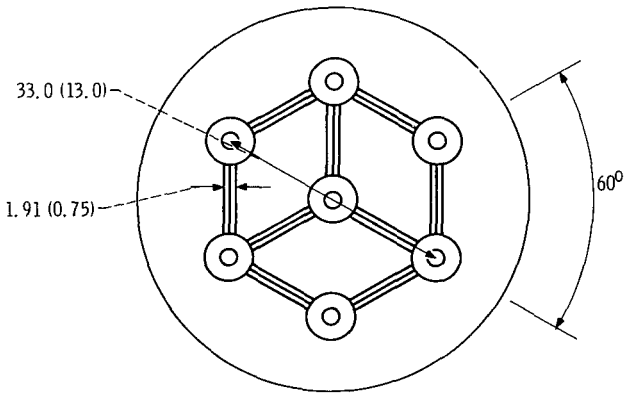

(c) Configuration D-3; blocked area ratio, 0.24.

Figure 17. - Swirl-can arrays. Dimensions are in centimeters (in.).

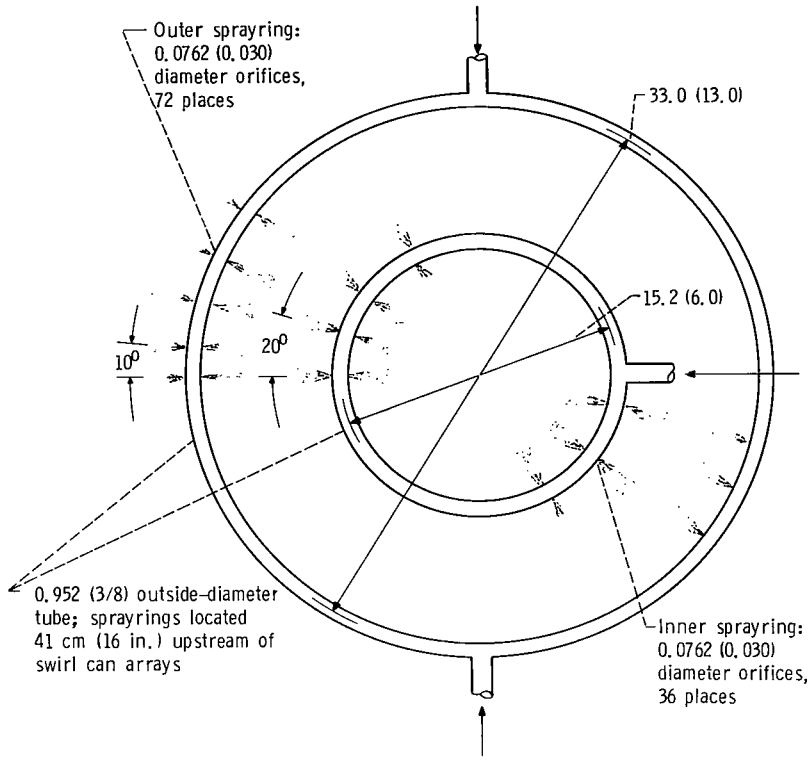

Figure 18. - Upstream fuel sprayrings for configurations D-2 and D-3. Dimensions are in centimeters (in.).

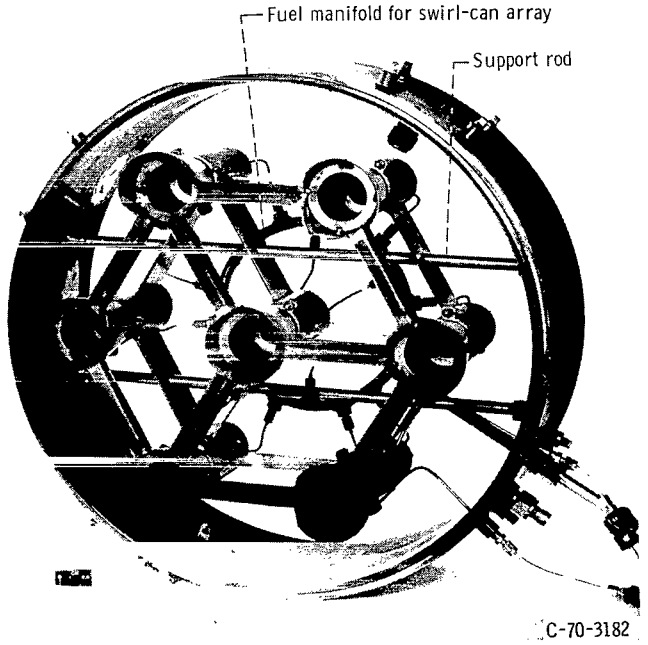

Figure 19. - Swirl-can array configuration D-3 (looking upstream).

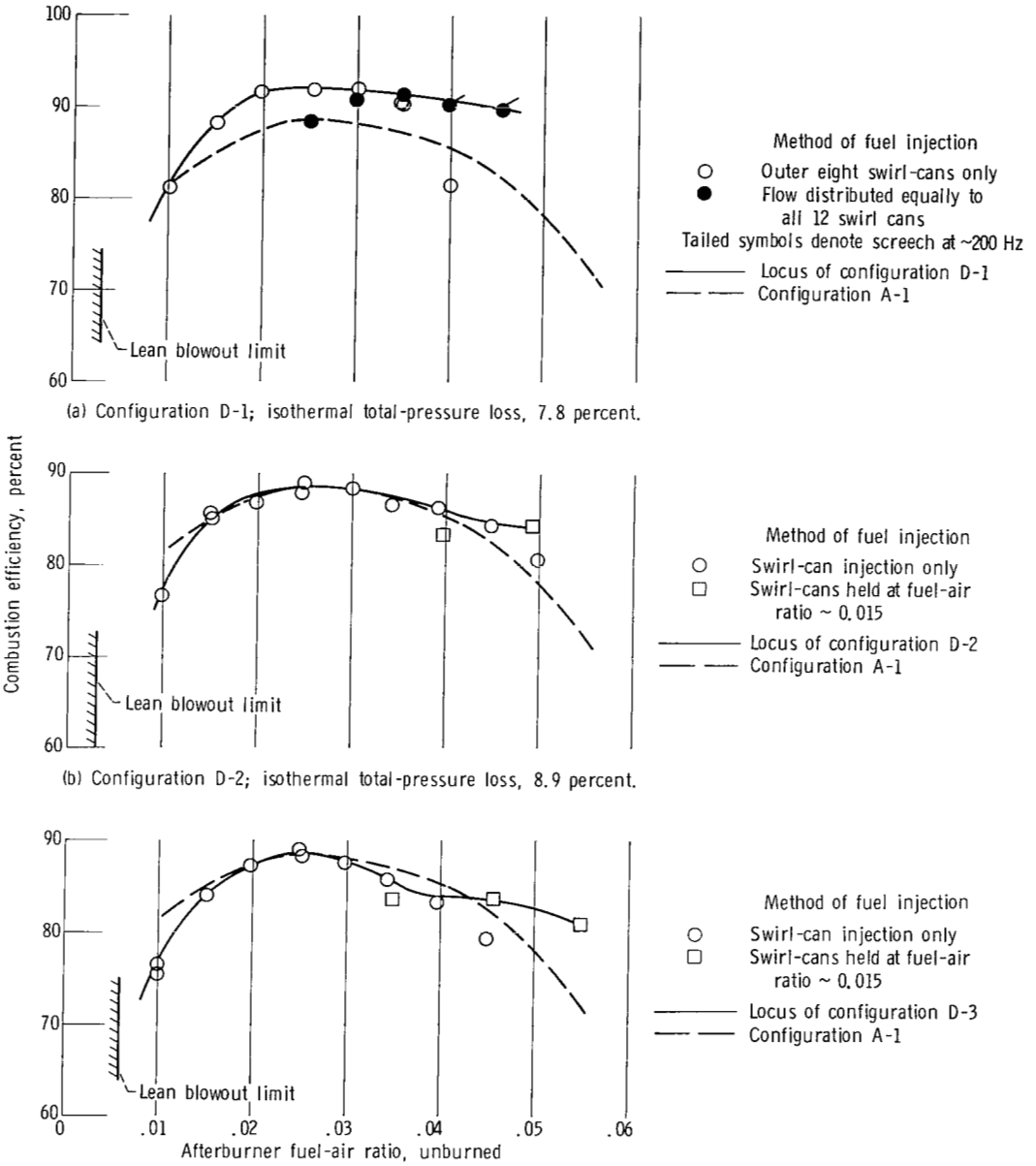

(a) Configuration D-1; isothermal total-pressure loss, 7.8 percent.

(b) Configuration D-2; isothermal total-pressure loss, 8.9 percent.

(c) Configuration D-3; isothermal total-pressure loss, 5.5 percent.

Figure 20. - Combustion efficiency of swirl-can arrays. Inlet conditions: temperature, 920 K (1200° F); pressure, 10.0 newtons per square centimeter (14.5 psia); velocity, 150 meters per second (500 ft/sec); preheater fuel-air ratio, 0.012.

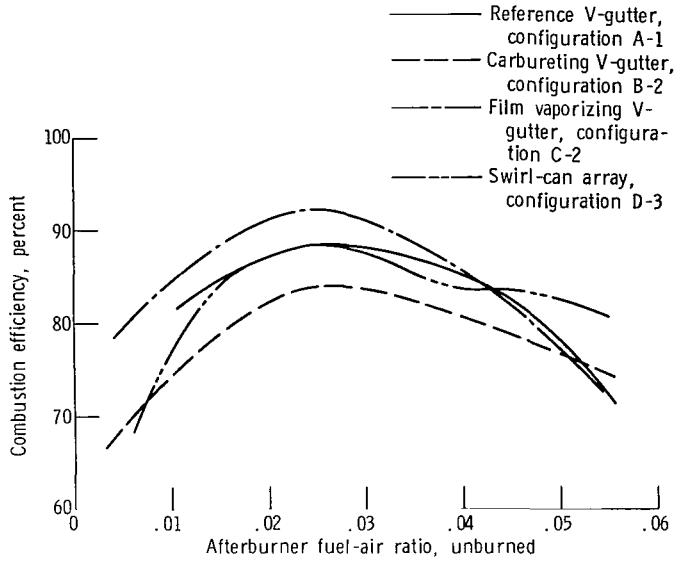

Figure 21. - Comparison of combustion efficiencies.

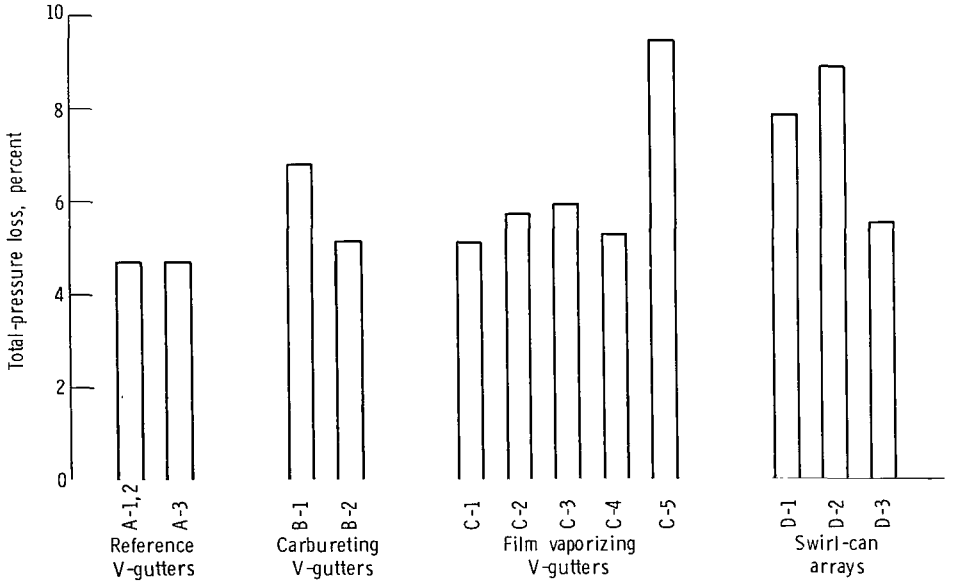

Figure 22. - Comparison of isothermal total-pressure losses at inlet Mach number of 0.27.

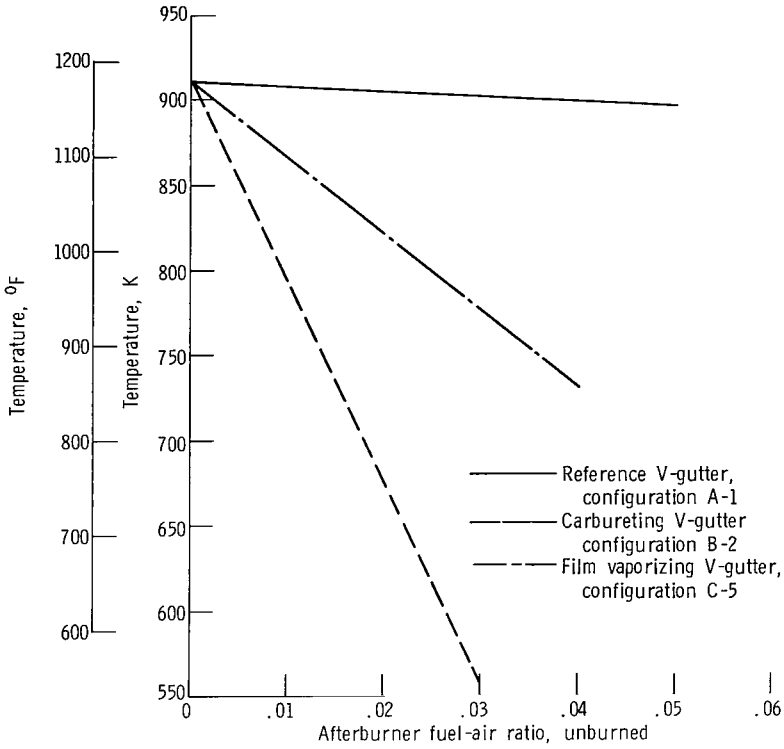

Figure 23. - Comparison of V-gutter skin temperatures.

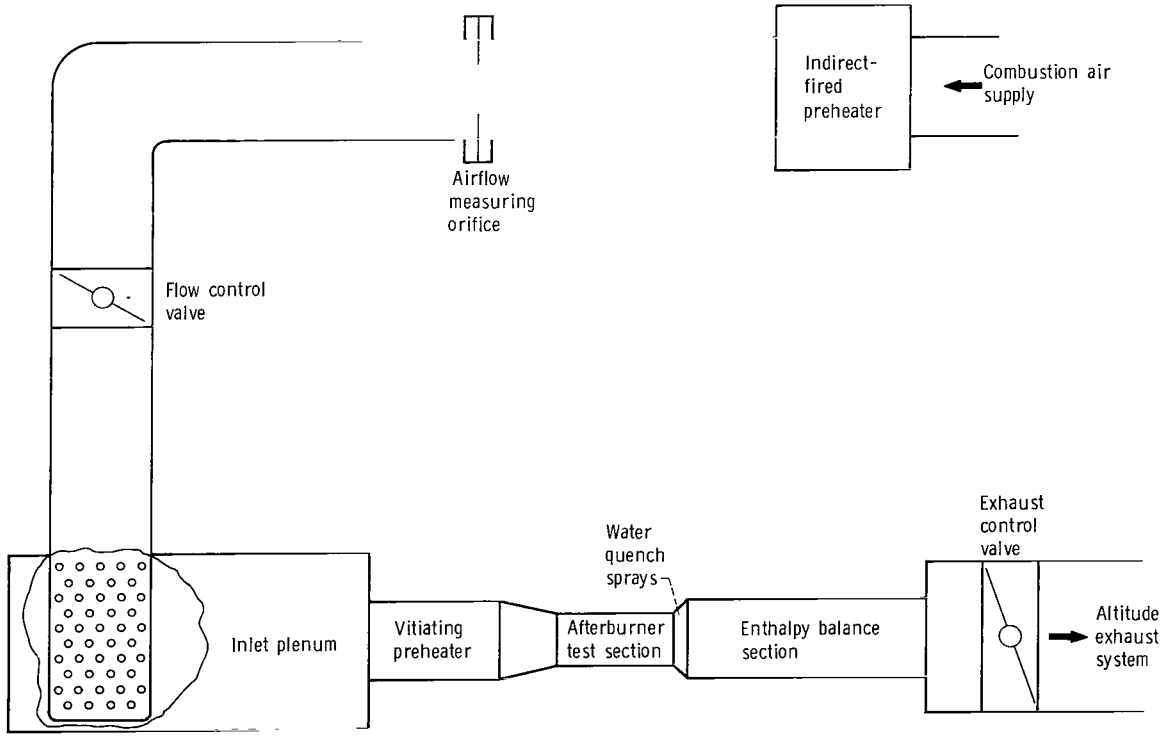

Figure 24. - Schematic diagram of afterburner test facility.

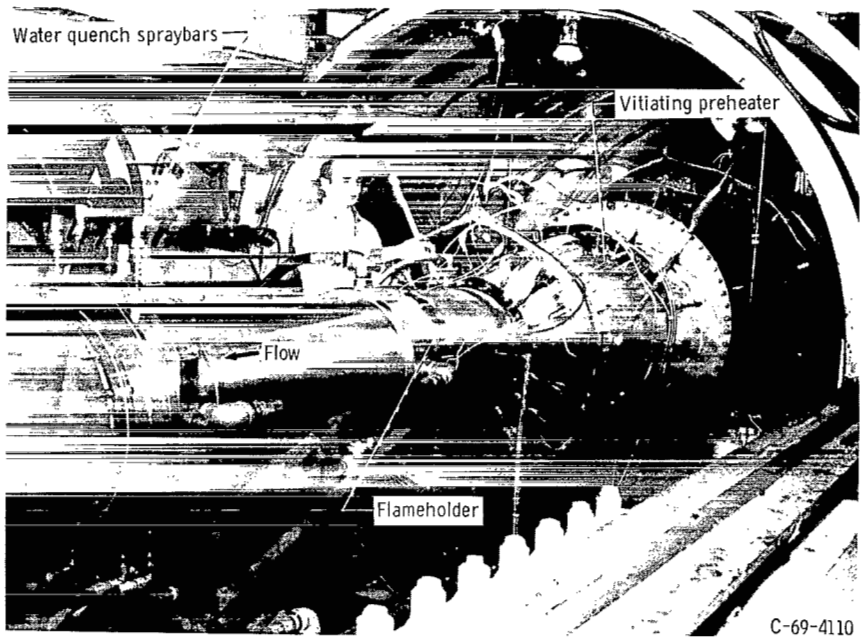

Figure 25. - View of afterburner test facility.

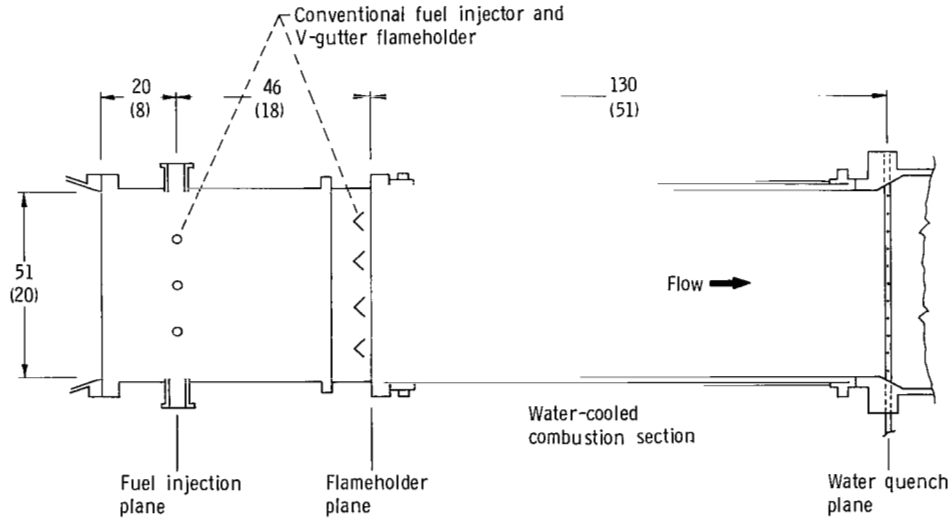

Figure 26. - Cross-section view of afterburner test section. Dimensions are in centimeters (in.).

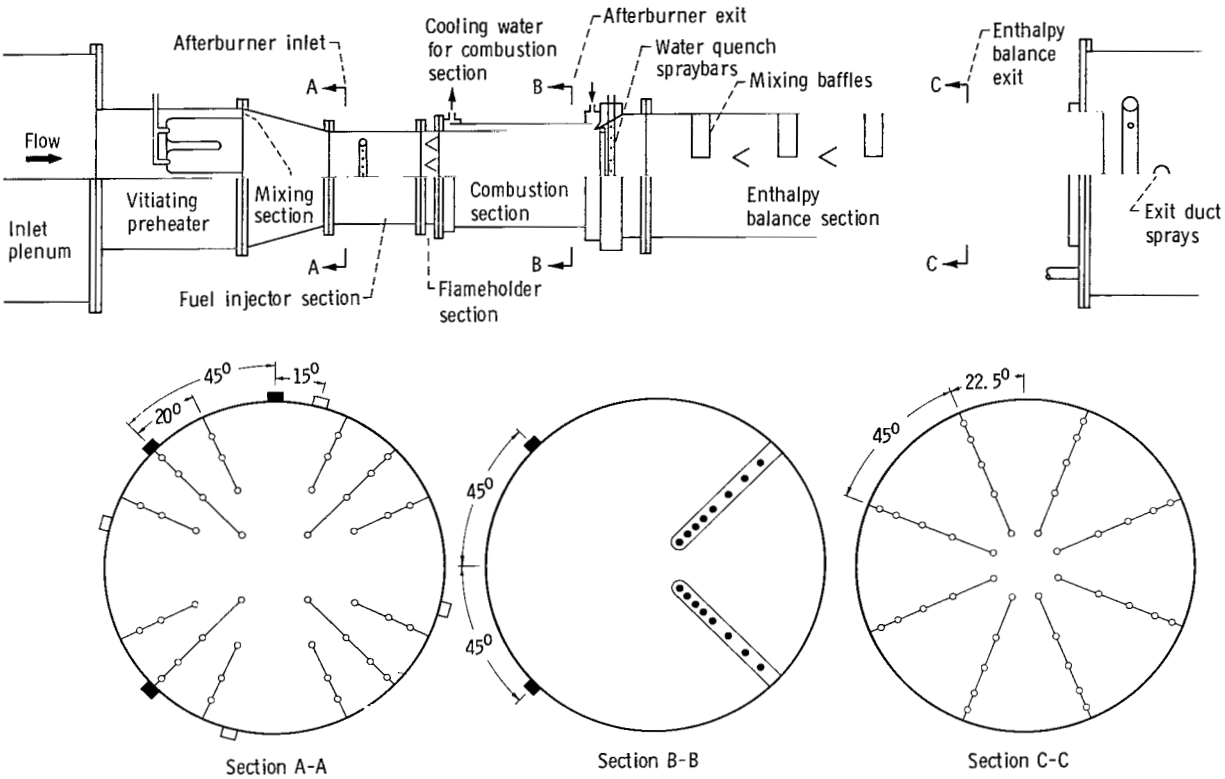

Figure 27. - Afterburner instrumentation.

017 001 C1 U 33 710730 S00903DS
DEPT OF THE AIR FORCE
WEAPONS LABORATORY /WLOL/
ATTN: E LOU BOWMAN, CHIEF TECH LIBRARY
KIRTLAND AFB NM 87117

"The aeronautical and space activities of the United States shall be conducted so as to contribute . . . to the expansion of human knowledge of phenomena in the atmosphere and space. The Administration shall provide for the widest practicable and appropriate dissemination of information concerning its activities and the results thereof."

—NATIONAL AERONAUTICS AND SPACE ACT OF 1958

NASA SCIENTIFIC AND TECHNICAL PUBLICATIONS

TECHNICAL REPORTS: Scientific and technical information considered important, complete, and a lasting contribution to existing knowledge.

TECHNICAL NOTES: Information less broad in scope but nevertheless of importance as a contribution to existing knowledge.

TECHNICAL MEMORANDUMS: Information receiving limited distribution because of preliminary data, security classification, or other reasons.

CONTRACTOR REPORTS: Scientific and technical information generated under a NASA contract or grant and considered an important contribution to existing knowledge.

TECHNICAL TRANSLATIONS: Information published in a foreign language considered to merit NASA distribution in English.

SPECIAL PUBLICATIONS: Information derived from or of value to NASA activities. Publications include conference proceedings, monographs, data compilations, handbooks, sourcebooks, and special bibliographies.

TECHNOLOGY UTILIZATION PUBLICATIONS: Information on technology used by NASA that may be of particular interest in commercial and other non-aerospace applications. Publications include Tech Briefs, Technology Utilization Reports and Technology Surveys.

Details on the availability of these publications may be obtained from:

SCIENTIFIC AND TECHNICAL INFORMATION OFFICE

NATIONAL AERONAUTICS AND SPACE ADMINISTRATION

Washington, D.C. 20546